

REPORT DOCUMENTATION PAGE

Form Approved
OMB No. 0704-0188

The public reporting burden for this collection of information is estimated to average 1 hour per response, including the time for reviewing instructions, searching existing data sources, gathering and maintaining the data needed, and completing and reviewing the collection of information. Send comments regarding this burden estimate or any other aspect of this collection of information, including suggestions for reducing the burden, to Department of Defense, Washington Headquarters Services, Directorate for Information Operations and Reports (0704-0188), 1215 Jefferson Davis Highway, Suite 1204, Arlington, VA 22202-4302. Respondents should be aware that notwithstanding any other provision of law, no person shall be subject to any penalty for failing to comply with a collection of information if it does not display a currently valid OMB control number.
PLEASE DO NOT RETURN YOUR FORM TO THE ABOVE ADDRESS.

1. REPORT DATE (DD-MM-YYYY)	2. REPORT TYPE FINAL	3. DATES COVERED (From - To) 03/02/2015-02/02/2018
-----------------------------	-------------------------	---

4. TITLE AND SUBTITLE A Power Efficient, Ultra Low Noise Amplification Mechanism in Semiconductor	5a. CONTRACT NUMBER
	5b. GRANT NUMBER N00014-15-1-2211
	5c. PROGRAM ELEMENT NUMBER

6. AUTHOR(S) Lo, Yu-Hwa	5d. PROJECT NUMBER
	5e. TASK NUMBER
	5f. WORK UNIT NUMBER

7. PERFORMING ORGANIZATION NAME(S) AND ADDRESS(ES) University of California, San Diego 9500 Gilman Drive, MC0934 La Jolla, Ca 92093	8. PERFORMING ORGANIZATION REPORT NUMBER 215C0A
--	--

9. SPONSORING/MONITORING AGENCY NAME(S) AND ADDRESS(ES) Office of Naval Research 875 N. Randolph Street, Suite 1425 Arlington, VA 22203-1995	10. SPONSOR/MONITOR'S ACRONYM(S) ONR
	11. SPONSOR/MONITOR'S REPORT NUMBER(S)

12. DISTRIBUTION/AVAILABILITY STATEMENT
Approved for Public Release: Distribution is Unlimited

13. SUPPLEMENTARY NOTES

14. ABSTRACT
Within this project, we have made significant progress in three areas:
(1) Confirm the underlying physical mechanisms of the cycling excitation process (CEP). To prove our theory, we have demonstrated excellent CEP device characteristics using amorphous silicon (a-Si) as the signal amplification medium.
(2) We have developed methods to realize the CEP effect to achieve record high detector performance, including demonstration of ultrahigh gain-bandwidth product and low noise of the detector.
(3) We have demonstrated CEP devices to detect single photons under low (8V) bias and room temperature.

15. SUBJECT TERMS

16. SECURITY CLASSIFICATION OF:			17. LIMITATION OF ABSTRACT UU	18. NUMBER OF PAGES	19a. NAME OF RESPONSIBLE PERSON Lo, Yu-Hwa
a. REPORT	b. ABSTRACT	c. THIS PAGE			19b. TELEPHONE NUMBER (Include area code) (858) 822-3429

Final Report: A Power Efficient, Ultra Low Noise Amplification Mechanism in Semiconductor

Within this project, we have made significant progress in three areas:

- (1) Confirm the underlying physical mechanisms of the cycling excitation process (CEP). To prove our theory, we have demonstrated excellent CEP device characteristics using amorphous silicon (a-Si) as the signal amplification medium.
- (2) We have developed methods to realize the CEP effect to achieve record high detector performance, including demonstration of ultrahigh gain-bandwidth product and low noise of the detector. Such attractive detector performance shows great promise for next generation imagers for defense and commercial applications.
- (3) We have demonstrated the ability of the CEP device to detect single photons under low (8V) bias and room temperature.

The details of the accomplishments are discussed in the following:

(1) Demonstration of cycling excitation process with disordered materials.

Since our first publication reporting the discovery of cycling excitation process in 2014, there has been skeptics about the existence of the claimed CEP mechanism or really a known mechanism revealed in a different manner. Through detailed modeling of the physical effect and experimental studies, we have obtained clear evidences of the existence of the CEP effect as a physical mechanism for signal amplification that has never been identified before. To prove such concept, we have designed a bold experiment to use disordered material such as amorphous silicon as the “gain medium” for the detector.

Based on all existing theories, disordered materials possess many properties that are against high performance photodetectors, compared to defect-free single-crystalline semiconductor materials. Some of the most obvious concerns for disordered materials include their very low carrier mobility and high defect density. It has been a common belief that high carrier mobility is necessary for any high-speed devices as mobility is a metric of the intrinsic speed for electron transport. Furthermore, it is believed that low material defect is required for low device noise based on the well-established Shockley-Read-Hall (SRH) recombination model. In the SRH model, defects are regarded as the sources for carrier recombination and generation-recombination noise. However, our theory has predicted that these so-called “defects” found in disordered materials can be favorable for photocurrent amplification, if properly engineered according to our proposed theory of CEP effect. We consider those “defect states” to be localized states that can enhance the Auger excitation for carrier multiplication because they help relax the quantum mechanical k-selection rule.

Based on our theory, we created a device with hydrogen-loaded amorphous silicon as the gain medium. The device structure consists of a thin (30nm) a-Si layer sandwiched by an ITO transparent electrode and n-Si substrate, as shown in Fig. 1. We adopted such a simple structure to eliminate possible side effects but the effect of the a-Si layer. The device shows very low dark current due to the high resistivity and relatively high bandgap (1.73 eV) of a-Si. Under 405nm illumination, the device produces gain of over 1000 under 4V bias (Fig. 2), showing that the carrier multiplication efficiency is orders of magnitude greater than impact ionization found in conventional avalanche photodiodes (APDs) made of high quality epitaxial semiconductors.

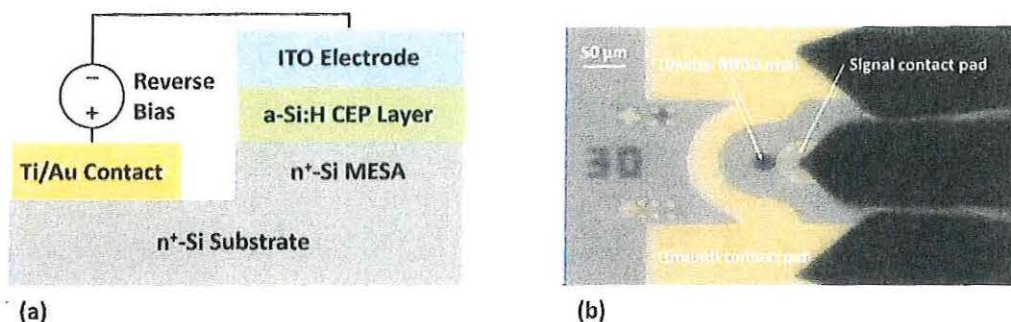


Figure 1. Device structure and design. a, Schematic diagram of a-Si CEP device structure with the material and function of each layer. The photodiodes operate under reverse bias. b, Device micrograph with ground-signal-ground (GSG) probe on the contact pads. The device active area is the 30 μm diameter circle. The signal contact pad is isolated from the substrate by a 200nm SiO_2 insulation layer.

The design is extremely exciting not only because it shows higher performance and signal amplification efficiency than impact ionization but more importantly, it overturns the conventional wisdom about disordered materials and the traditional notion for suitable for optical detection. The latter has tremendous ramifications for imaging and communications. It suggests that many disordered materials, including amorphous semiconductors, dielectric materials, and polymers can all be used as effective gain media to efficiently amplify photocurrent, even though these materials may have extremely low mobility (e.g. $< 1/1000$ of crystalline silicon) and a large number of “defects” in conventional sense.

We have further shown that it is important to engineer the localized states in disordered materials to produce favorable CEP effect. Using a-Si as an example, the “desirable localized states” are those states extended from the edge of the conduction and valence band, caused by the lack of long range order of the material. On the other hand, there are “harmful” states around the middle of bandgap, caused by the dangling bonds of silicon. These states are responsible for SRH recombination and can suppress the gain and quantum efficiency because carriers trapped in those deep states cannot be excited by phonon absorption or tunneling. Therefore, it is crucial that we

remove/minimize the density of such deep levels using hydrogen to passivate the dangling bonds of silicon. We have further shown that by adding a small percentage of carbon, the passivation of dangling bonds can be more effective because the gas source of carbon, methane, generates atomic hydrogen more effectively than silane. In addition, because of carbon's much lighter mass than silicon, carbon in a-Si produces more energetic phonons with strong electron-phonon coupling to enhance the amplification process. These effects can be shown from the characteristics of voltage dependent gain in Fig. 2.

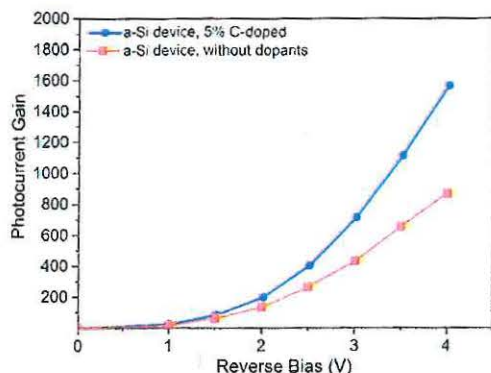


Figure 2. Photocurrent gain for a-Si CEP photodiodes. DC photo-current gain of a carbon-doped and an intrinsic a-Si:H CEP photodiode. Both photodiodes have a 30 μ m diameter photosensitive area. Unity gain is referred to zero bias photocurrent having only the built-in field in the CEP medium.

(2) Demonstration of excellent high-speed and noise characteristics of a-Si CEP detector.

The excellent DC characteristics for CEP device with carbon-doped a-Si have motivated us to investigate their high frequency and noise characteristics. This is particularly interesting since our earlier work with heavily doped and compensated Si p/n junction device has shown low frequency (< 1MHz) gain cutoff. We have hypothesized that such low frequency gain cutoff was due to "carrier hopping" in regions that have low E-field (i.e. outside the depletion region), rather than the intrinsic property of the CEP effect. If this is true, then the low-frequency gain cutoff should not occur to a-Si as the gain medium since the entire a-Si layer (30nm total thickness) is under high electric field. Furthermore, our theorem further predicts that the device will possess excellent noise characteristics because of the ultrathin gain medium compared to conventional APDs and the phonon-mediated process as a built-in negative feedback mechanism.

Figure 3 shows the gain dependence on the modulation frequency for 405nm laser light. At -4V bias, the 3dB cutoff frequency is around 1.5GHz. For a gain of 1500, this gives rise to a gain-bandwidth product of 2.25THz. The gain bandwidth product is about 6 times greater than the best result for APDs and set the world record for any photodetectors. We also notice from Fig. 3 that the 3dB cutoff frequency is nearly independent of the bias voltage, suggesting that the cutoff

frequency is likely due to the RC limit of the 30 μ m diameter device instead of the intrinsic response of the CEP effect. The result has provided unequivocal evidence that the CEP device can possess high frequency response and the previously observed gain roll-off under 1MHz was due to other side effects (e.g. carrier hopping in low-field regimes). The result also proves that mobility is not a relevant material parameter for the speed of the device concerning the CEP effect.

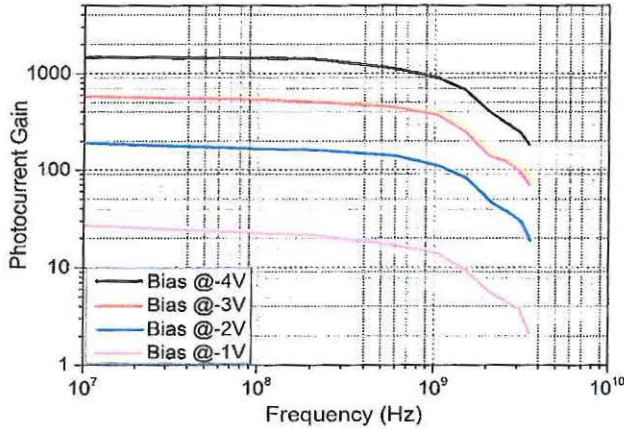


Figure 3. Frequency dependence of gain for a carbon-doped a-Si:H CEP photodiode. The AC photocurrent gain versus the laser power modulation frequency is plotted under four different reverse bias voltages. Low frequency (below 10MHz) gains are close to DC gain values. The 3dB cutoff frequency is about 1.5GHz. Above 1.5GHz, the AC gain decreases at a rate of around 20dB/decade.

Finally, we characterize the noise properties of a-Si CEP detectors. For devices with high internal gain, the dominant noise is the shot noise and is best characterized by the excess noise factor. The excess noise factor quantifies the extra shot noise caused by instantaneous gain fluctuation. For conventional APDs, the physical model predicts that the excess noise factor increases almost linearly with gain in the high gain regime.

To answer many questions from the reviewers of our submitted paper about the method of noise measurement, in the following we elucidate our noise measurement setup and the method of deriving the excess noise factor in detail.

We measured the device noise using a DC laser source and a low noise amplifier (LNA) and RF spectrum analyzer, as shown in Fig. 4. We measured the noise at 70MHz because the frequency is high enough to avoid 1/f noise and low enough compared to the gain-bandwidth product of the device. Even for a device with 80 to 100 GHz gain-bandwidth product (e.g. commercial Si APDs), the device is capable of producing gain of the order of 1000 at 70 MHz.

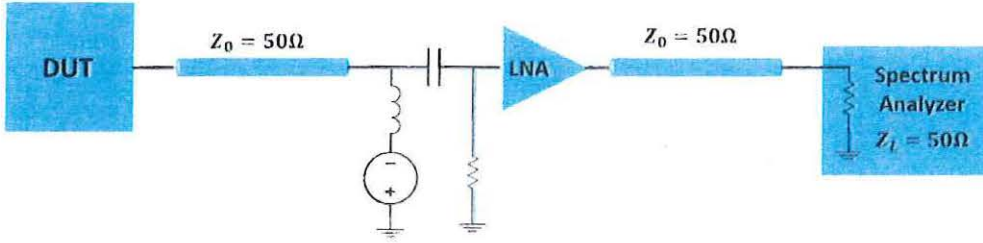


Figure 4. Schematic circuit diagram for noise measurement.

Assuming shot noise is dominant and dark current experiences the same amount of gain as photocurrent, we have,

$$\sigma_s^2 = 2qG^2F_A(RP_{in} + I_d)\Delta f = 2qG^2F_A(I_{ph0} + I_d)\Delta f$$

$$\sigma_d^2 = \sigma_s^2(P_{in} = 0) = 2qG^2F_AI_d\Delta f$$

We denote,

F_A : Excess noise factor.

I_d : Primary dark current without amplification.

I_{ph0} : Primary photo-current.

σ_s^2 : Noise power in light-on condition.

σ_d^2 : Noise power in dark condition.

Measure noise under light-on and dark conditions and take the difference

$$\sigma_s^2 - \sigma_d^2 = 2qG^2F_AI_{ph0}\Delta f = 2qGI_{ph}F_A\Delta f$$

$$F_A = \frac{\sigma_s^2 - \sigma_d^2}{2qGI_{ph}\Delta f} \quad (1)$$

To obtain (1), we have used the relation: $I_{ph} = GI_{ph0}$.

What spectrum analyzer measures, however, is the Noise Power Spectrum Density (NPSD) of the amplified device noise with some cable loss and added noise by the LNA. So we further denote:

$NPSD_S$: Measured Noise Power Spectrum Density in light-on condition.

$NPSD_d$: Measured Noise Power Spectrum Density in dark condition.

N_a : Added noise from the Low Noise Amplifier.

G_{LNA} : Power gain of the Low Noise Amplifier.

G_{cable} : Power “gain” (loss) due to the cable and bias tee frequency response. The power loss by the 50Ω in-shunt resistor is also considered in this term.

Considering the DUT as a current source and the input impedance of the LNA is also $50\Omega = R_L$. Therefore, the reading from the spectrum analyzer can be presented as,

$$NPSD_s = \frac{\sigma_s^2 \cdot G_{cable} \cdot R_L \cdot G_{LNA} + N_a}{\Delta f}$$

$$NPSD_d = \frac{\sigma_d^2 \cdot G_{cable} \cdot R_L \cdot G_{LNA} + N_a}{\Delta f}$$

Taking the difference, we shall see the added noise from the LNA is canceled.

$$NPSD_s - NPSD_d = (\sigma_s^2 - \sigma_d^2) R_L G_{cable} G_{LNA} / \Delta f$$

$$\frac{NPSD_s - NPSD_d}{G_{LNA} G_{cable} R_L} = \frac{\sigma_s^2 - \sigma_d^2}{\Delta f}$$

At last, substituting the above relation into (1), we calculate Excess Noise Factor (F_A) from measured NPSD,

$$F_A = \frac{NPSD_s - NPSD_d}{G_{LNA} G_{cable} R_L} \cdot \frac{1}{2qGI_{ph}} \quad (1)$$

The results of excess noise measurement are shown in Fig. 5. The excess noise factor for the commercial Si APD shows the typical characteristics fitted well to the McIntyre’s noise model. On the other hand, the excess noise factor of the a-Si CEP device is significantly lower than the APD noise. The noise for the CEP device at gain below 200 is too low to measure due to the noise floor (-171 dBm/Hz, which is 3dB above the thermal noise limit) of our test system. Notably the result is particularly striking as disordered materials have been considered inherently noisy due to their high concentration of “defects”. However, for CEP devices, the ultrathin gain medium, made possible by the high Auger excitation efficiency, and the phonon mediated process have greatly suppressed the noise, resulting in a much lower excess noise than traditional APDs.

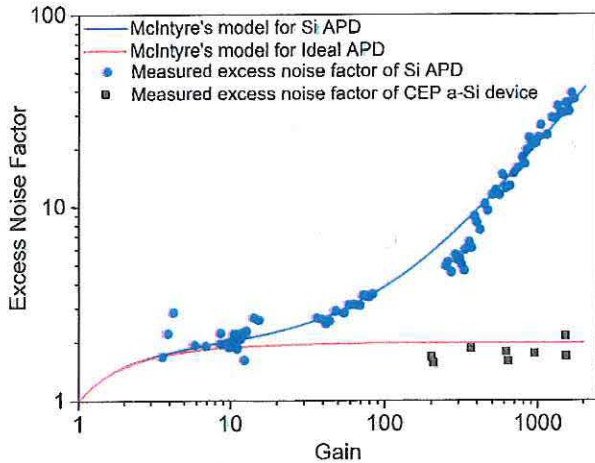


Figure 5. Excess noise factor dependence on gain. The photocurrent gain dependence of excess noise factor for a commercial Silicon APD and a C-doped a-Si:H CEP device. The experimentally measured excess noise factor of a commercial Silicon APD (blue dots) matches McIntyre's model¹¹ for Silicon APD well (blue curve). The excess noise factor measured for the carbon-doped a-Si:H CEP device is shown as discrete black squares, which are close to the noise properties of an ideal photocurrent amplifier (red curve).

(3) Demonstration of single photon response with CEP detectors.

With the device in Fig.1 that produces a gain-bandwidth product of over 2 THz, we have been able to achieve photon counting characteristics at 500 MHz without any quenching circuit. Figure 6 shows the output of an a-Si CEP detector under a sinusoidally modulated 405nm laser at 500MHz. The light intensity is attenuated to achieve the designed number of photons within a 2ns cycle. The device can respond to signals when the light intensity is reduced to as few as 3 photons per cycle. Figure 7 shows the histogram of the detector response under different photon numbers within each cycle. It shows that the detector in Fig. 1 can reliably detect 5 photons. Below this level the sensitivity is limited by the gain of the device and the noise of the external amplifier. Nonetheless, this is the world's fastest semiconductor photon counter operating at low bias voltage (<5V) without any (passive or active) quenching circuit.

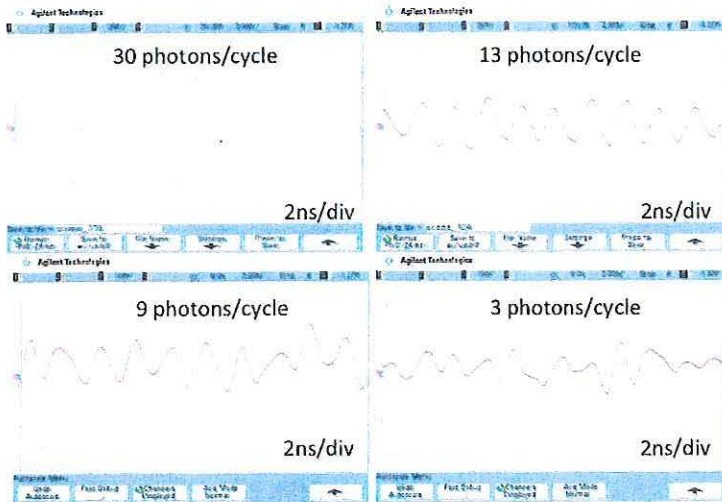


Figure 6. Dependence of CEP detector output on the number of input photons per cycle at 500MHz.

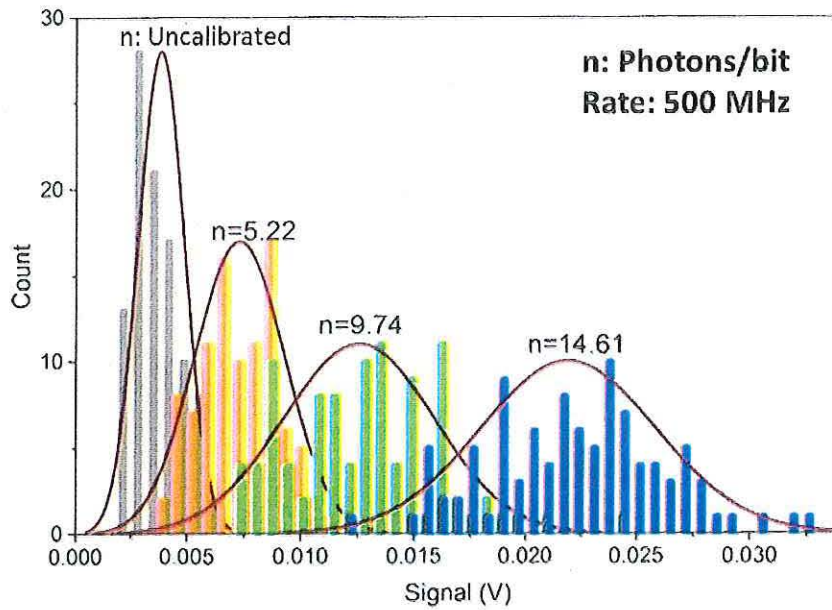


Figure 7. Detector response for photon counting. The numbers above each histogram refer to the average number of photons within each 2ns cycle.

In spite of the impressive device characteristics, the simple device in Fig. 1 is not able to obtain single photon response due to the insufficient gain of the a-Si layer alone. To further improve the device characteristics, we put a single crystalline Si p/n junction in series with the 35nm a-Si layer. The device now has a so-called MAGIC (multiple amplification gain and internal control) design we invented years ago. With the new structure, the device is capable of detecting single photons at GHz rate. The device response to two subsequent single photons arrived in 2 ns is shown in Fig. 8.

To show the true response of the device, we have replaced the 1GHz low noise amplifier with a wide band 30GHz amplifier. The impulse response to single photons shows a output pulse as fast as 150ps. Again, the device requires no quenching circuit and is not limited by recovery time as conventional Geiger mode SPADs. Therefore, we have shown promising results for ultrafast single photon detectors operating at multi GHz frequencies.

Our work not only sets the new world records in detector sensitivity and speed, but also demonstrates the feasibility for a new generation of detectors operated under a new physical principle, with ultrahigh sensitivity and speed well beyond any existing semiconductor photodetectors.

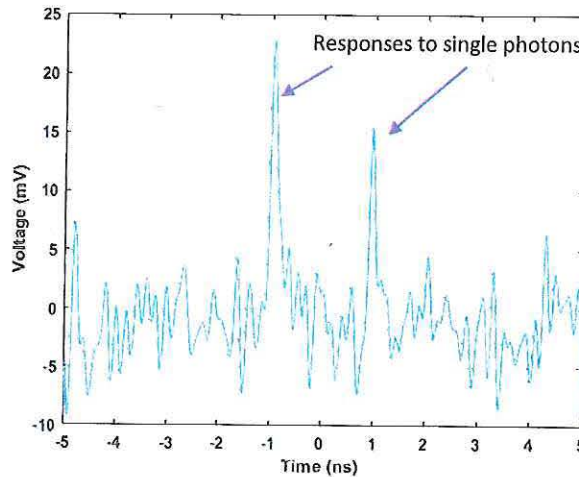


Figure 8. Response to single photon by a detector consisting of a s-Si (35nm) layer and a single crystalline Si p/n junction. The device is biased at 8V and shows 40% quantum efficiency at 518nm wavelength.